 Egyptian J. Desert Res., **73**, No. 2, 629-653 (2023)

GEOCHEMICAL, NATURAL RADIOGENIC AND ISOTOPIC IMPLICATIONS FOR NUBIAN SANDSTONE GROUNDWATER ASSESSMENT IN KHARGA OASIS, WESTERN DESERT, EGYPT

Eissa, Mustafa A.
Department of Hydrogeochemistry, Desert Research Center, Cairo, Egypt
E-mail: mustafa.eissa#@drc.gov.eg, mostafaa75@hotmail.com

Groundwater in the Kharga Oasis, located in the Western Desert of Egypt, is an essential resource for the local population. The Oasis is fed by the Nubian Sandstone Aquifer (NSA) of the Cretaceous age. This aquifer is one of the world's largest reservoirs, which provides fresh water for drinking, irrigation, domestic use, and industrial purposes. The NSA possesses four bearing zones; Zone A, Zone B, Zone C, and Zone D, which are separated by clay confining layers. The total penetration depth ranges from 12.5 to 800 meters, and the aquifer is underlain by granitic and basement rocks. The groundwater temperature ranges between 18 to 36.8°C, where high temperatures have been detected in the deeper zones (C and D), indicating geothermal activity. Generally, the quality of NSA water is fresh to brackish water types; however, the deeper aquifer zones (C and D) mainly contain freshwater. The concentrations of the trace elements and the natural radioactive nuclei (Rb, Pb, ^{232}Th, ^{238}U, and Sr) in the NSA waters are insignificant and far below the permissible drinking limits, and they are mainly coming from the geogenic source due to leaching of aquifer matrix. The stable isotopes (δ^{18}O and δ^{2}H) show great insights for recharge and salinization sources. The δ^{18}O ranges from -11.96 to -6.11‰, while δ^{2}H ranges between -83.5 to -67.7‰, indicating that the groundwater in the NSA is fossil water (paleo-meteoric origin) as the aquifer was recharged during the paleo heavy pluvial periods. Accordingly, the groundwater in Kharga Oasis is a paleo nonrenewable resource whose quality has been threatened mainly by geogenic natural pollution, agricultural activity, and over-exploitation.

Keywords: Hydrogeochemistry, stable isotopes, radioactive nuclei, geochemical modeling, Kharga Oasis

INTRODUCTION

Groundwater is the primary source of freshwater all over the world and is mainly used for different purposes, including drinking and agriculture (Mondal et al., 2022; Sinha et al., 2023 and Mishra et al., 2023). The Western Desert of Egypt is a hyper-arid region with a dominant climate of scarce rainfall and high evaporation. The groundwater in the Nubian Sandstone aquifer (NSA) occurs under confining conditions and represents the sole sustainable source of freshwater (King-Okumu et al., 2021). The NSA aquifer has a tremendous regional extension, extending into Egypt, Chad, Sudan, and Libya. In Kharga Oasis, the Nubian Sandstone Aquifer (NSA) is discharged mainly through natural springs and deep-drilled wells. Aquifer exploitation has been started for irrigation purposes since 1959 through many deep-drilled wells. The groundwater withdrawals increased to 1.7 million cubic meters from 1960 to 1980, with more than 86.7% consumed for irrigation (Lamoreaux et al., 1985 and Saber et al., 2022). The overexploitation declined the groundwater level from 40 to 80 m below the ground surface from 1967 to 2007 (Mekkawi et al., 2017). Hydrological, atmospheric, climatic, topographical, and lithological factors are all natural influences on groundwater quality (Islam et al. 2017; Mukate et al., 2020 and Uddin et al., 2023). In the last decades, the groundwater quality of the NSA has been degraded due to high groundwater abstraction and declining water levels. In Kharga Oasis, the groundwater chemistry is mainly influenced by water-rock interaction, recharge source(s), and aquifer hydraulic parameters (Saber et al., 2022). Additionally, Sherif and Sturchio (2021) reported that the natural radioactivity of the NSA impairs groundwater quality and threatens health risks for adults and infants. The concentration and mobility of radioactive elements in groundwater depend mainly on the residence time between the aquifer matrix, groundwater flow path, redox potential, and mixing with different waters (Divers et al., 2014 and Ammar et al., 2020). The NSA is a multi-layered aquifer where each layer has unique geochemical characteristics and a dynamic flow system. Therefore, the major ions chemistry, stable isotopes, and radioactive elements have been measured in the groundwater to determine the factors affecting groundwater quality, to expect the primary source(s) of aquifer recharge, and to investigate the mobility and the health risk of radioactive elements in groundwater of the NSA.

1. The Study Area

Kharga Oases is in the Western Desert of Egypt and lies between latitudes 24.7 to 25.8 North and longitudes 30.4 to 30.7 East (Fig. 1 a and b). Kharga is the largest oasis in the Western Desert, occupying about 12,000 km^2, and it represents an oval shape that extends from North to South. The Oasis is bounded from the north by the Abu Tartur Plateau and from the east by the Thebes Plateau. It was reported that the highest temperature was recorded in summer during July (50ºC), while the lowest temperature was recorded in January (20ºC), and the relative humidity ranges from 30% (summertime) to 56% (wintertime). Annual rainfall ranges from 0.1 to 1 mm/year (Younis et al., 2016). The Oasis occupies rocks ranging in age from the Pre-Cambrian to the Quaternary (CONOCO, 1987). It is bounded from the North and East by the Eocene limestone Plateau with an elevation of about 550 m above the sea level (El-Sankary, 2002). The groundwater generally flows from the southwest toward the northeast (Hellström, 1940 and Mahmod et al., 2013), and the aquifer is mainly discharged through springs' shallow and deep-drilled wells. The Nubian Sandstone aquifer consists of alternative beds of sandstone and sandy clay layers intercalated with impermeable shale interbeds. The aquifer thickness ranges from 300 to 700 m, where the thickness mainly increases towards the North (Boukhary et al., 2013 and Younis et al., 2016). The aquifer is divided into four zones: A (Taref Fm), B (Sabaya Fm), C, and D (Six Hills Fm) (Diab, 1978; RIGW, 2006 and Abd Allah, 2013) (Fig. 1 a and b and Fig. 2). Zone A is the uppermost layer, composed mainly of coarse sandstone with intercalation of gravel, limonite, muscovite, pyrite, and glauconite. Zone B is mainly coarse sandstone stained with iron ore, while Zone C is subangular to the surrounding sandstone layer. Zone D rests unconformably over the basement rocks and is composed of white, yellow, pale red, and coarse sandstone with gravel (Younis et al., 2016) (Fig. 1 a, b, and 2).

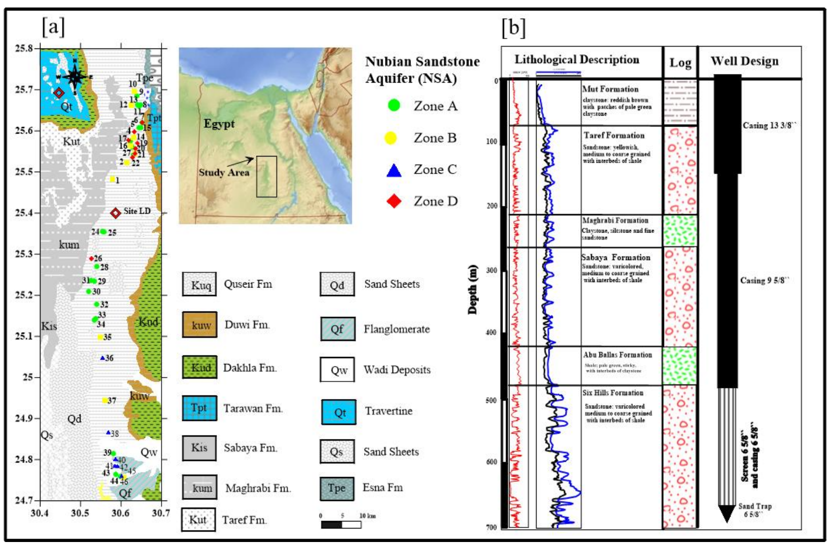

Fig. (1). a. Geological map of Kharga Oasis (Klitszch et al., 1987), **b.** Lithological description obtained from Gama Ray and Sp-Resistivity at site LD.

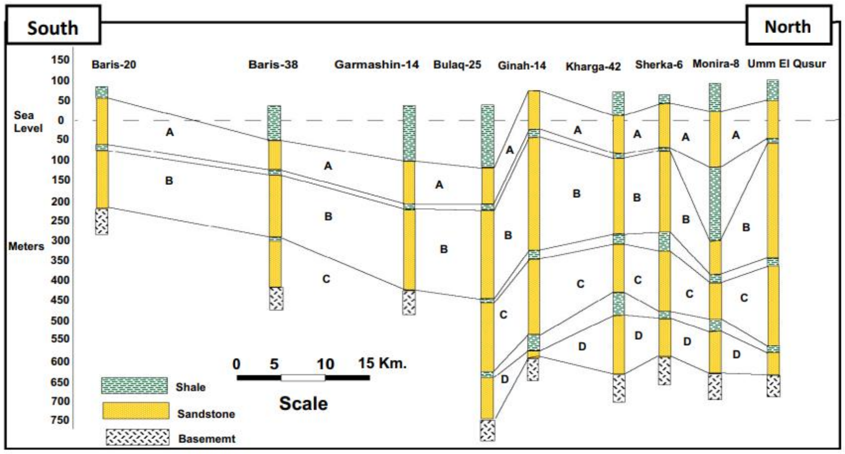

Fig. (2). Hydrogeological Cross Section North-South for Kharga Oasis (Abd Allah, 2013 and Younis et al., 2016).

The aquifer is dissected by a set of faults related to the fracturing of the Nubian system and represents an impermeable barrier to the lateral flow of groundwater (Lamoreaux et al., 1985). Two major fault systems dominated the Kharga Oasis; one extends northwest of Ym Qusur to Garmashin, and the second parallels the Thebes plateau escarpment. Based on the FAO report, about 9700 acres are cultivated in Kharga Oasis, and 22,000 acres are considered land for wild vegetation (FAO, 1977). The Nubian aquifer in has been over-exploited due to an unmanaged higher withdrawal rate. The groundwater extractions led to a decline in the groundwater level by about 33 meters in the Garmashine area and 3 meters at Baris (Soliman, 2013).

MATERIALS AND METHODS

In May 2022, 46 groundwater samples were collected from the NSA from wells varying in penetration depth and tapping different layers (Fig. 1). The samples were collected from continuously exploited wells in 500 ml polyethylene bottles previously rinsed with deionized water. The bottles were cleaned two to three times with the water obtained from the wells *in situ*. The groundwaters' temperature, pH, and electrical conductivity were measured in the field sites using Hanna HI 9813-61 portable pH/EC/TDS/temperature meter with a calibration check. The major ions (Ca^{2+}, Mg^{2+}, Na^{+}, K^{+}, SO_4^{2-}, and Cl^{-}) were determined using the IC-chromatograph (Thermo Scientific Dionex ICS-1100) at Desert Research Center water laboratory (Table 1). Alkalinity has been determined by titration against H_2SO_4 phenolphthalein and methyl orange as indicators (Hem, 1985). The stable isotopes $\delta^{18}O$ and $\delta^{2}H$ were determined at the UC DAVIS stable isotope facility using CO_2-H_2O and H_2-H_2O equilibration method on the Gas Bench-IRMS with a Delta Plus XL isotope-ratio mass spectrometer (Thermo-Finnigan, Bremen, Germany) (Coplen et al., 1991 and Coplen, 1995). The standard for measuring the isotopic ratios for $\delta^{18}O$ and $\delta^{2}H$ was calibrated against the IADA reference water (VSMOW). Precision for water samples at natural abundance is typically ±0.2‰ for $\delta^{18}O$ and ±2.0‰ for $\delta^{2}H$. The radioactive elements in groundwater have been determined using the iCAP TQ and a multi-standard solution of Rb, Sr, ^{232}Th, and ^{238}U at the Egyptian Nuclear Authority laboratory in Cairo. The concentrations for radionuclides in groundwater have been reported in ppb, and the intensity average is in cps (Table 2). The geochemical NETPATH model has been used to evaluate the geochemical mass transferred due to water-rock interaction within the flow path and estimate physical parameters, including mixing and evaporation (Plummer et al., 1992). The Statistical Package for the Social Sciences (SPSS) software developed by IBM (Argyrous, 2011) has been used to investigate the controlling factors governing the radionuclides and factors leading to groundwater salinization in the NSA.

RESULTS AND DISCUSSIONS

1. Major Ions and Salinity Distribution

The electrical conductivity of groundwater (EC in µMohs/cm) measures the ability of water to conduct the electrical current. It is directly proportional to the amount of dissolved salts in water. The EC of groundwater in Kharga Oasis ranges between 330 (well 26) to 8360 µMohs/cm (well 33) with an average value of 1199 µMohs/cm. The total dissolved solids (TDS, mg/L) of groundwater samples ranges between 197 (well 1) and 5738 mg/L (well 33), with an average value of 436 mg/L (Fig. 3). The dissolved calcium concentrations in groundwater samples range from 7 mg/L (well 37) to 380 mg/L (well 18) with an average value of 62 mg/L, while the dissolved magnesium ranges between 9 mg/L (well 1) and 341 mg/L (well 18) with an average value of 61 mg/L. Sodium records the highest concentrations of the dissolved major cations in groundwater, ranging from 12 mg/L (well 26) to 1350 mg/L (well 33), while potassium records the lower concentrations, where it ranges from 15 mg/L (well 36) to 155 mg/L (well 33). The bicarbonate records the lowest concentrations of the dissolved major anions, ranging between 0 mg/L (well 4) and 351 mg/L (well 18), with an average value of 160 mg/L. The sulfate records the highest concentrations of the dissolved major anions. It ranges from 13 mg/L (well 8) to 2750 mg/L (well 4), with an average value of 268 mg/L. Additionally, chloride records higher concentrations, ranging between 44 mg/L (well 13) and 2719 mg/L (well 33), with an average concentration of 211 mg/L.

Table (1). Chemical and isotopic data for groundwater samples in Kharga Oasis area.

No	Aquifer Zone	Aquifer	pH	TDS	Ca	Mg	Na	K	CO_3	HCO_3	SO_4	Cl	$\delta^{18}O$	δ^2H
					ppm								(‰)	
3	**A**	Nubian Sandstone Aquifer (NSA)	7.9	312	34.8	15.8	46	30	0.0	166.9	36.0	65.8	-	-82
4	**A**		8.15	3834	347.8	184.9	1015	63	0.0	0.0	2750.0	921.1	-8.78	-71.9
5	**A**		8.21	424	26.1	23.8	95	19	0.0	229.5	80.0	65.8	-	-81.1
6	**A**		8.22	469	26.1	37.0	90	31	0.0	250.3	50.0	109.7	-	-80.7
8	**A**		8.01	281	34.8	21.1	26	34	0.0	173.9	12.6	65.8	-	-82
9	**A**		7.95	708	34.8	60.7	74	47	0.0	159.9	323.9	87.7	-	-82.2
11	**A**		8.01	395	26.1	31.7	35	36	0.0	153.0	124.5	65.8	-	-82.1
13	**A**		8.25	363	21.7	29.1	44	29	0.0	191.2	100.0	43.9	-	-81
18	**A**		8.34	4544	380.4	341.2	660	92	0.0	351.2	2280.0	614.0	-9.92	-77.8
23	**A**		8.35	914	43.5	72.6	150	27	0.0	264.3	291.3	197.4	-	-81.3
24	**A**		8.1	1924	173.9	211.3	136	87	0.0	281.6	912.0	263.2		
25	**A**		7.92	1269	73.9	107.0	100	120	0.0	139.1	513.8	285.1	-	-79.9
28	**A**		8.4	1585	113.0	204.3	80	66	0.0	31.3	864.9	241.2	-	-81.4
29	**A**		8.35	552	43.5	63.4	55	36	0.0	111.3	79.5	219.3	--	--
30	**A**		7.9	627	38.4	71.5	60	36	0.0	219.1	70.5	241.2	-	-76.6
31	**A**		7.8	376	29.0	39.6	20	35	0.0	100.8	70.8	131.6	-11.1	-81.8
32	**A**		7.95	322	26.1	33.5	18	33	0.0	100.8	52.1	109.7	-10.7	-80.1
33	**A**		8.21	5738	333.3	237.7	1350	155	0.0	114.7	885.5	2719.3	-6.11	-67.7
34	**A**		8.22	476	54.3	33.0	45	26	0.0	100.8	92.2	175.4	-	-81.4
39	**A**		8.19	288	25.6	28.0	26	28	0.0	104.3	18.8	109.7	-	-80.5
43	**A**		8.15	374	45.9	23.5	32	26	0.0	86.9	94.0	109.7	-	-80.1
44	**A**		8.21	459	65.2	26.4	51	20	0.0	76.5	149.0	109.7	-10.8	-81.6
1	**B**		8.22	197	13.0	9.0	23	34	0.0	41.7	20.0	76.8	-	-79.9
2	**B**		8.35	374	34.8	21.1	40	33	0.0	159.9	100.0	65.8	-	-76.7
10	**B**		8.15	377	21.7	29.1	48	32	0.0	201.7	80.0	65.8	-	-83.5
12	**B**		8.21	396	21.7	37.0	45	34	0.0	198.2	93.3	65.8	-11.2	-82.5
14	**B**		8.23	613	34.8	37.0	97	29	0.0	239.9	229.7	65.8	-	-80.8
16	**B**		8.15	411	34.8	42.3	40	30	0.0	191.2	81.0	87.7	-11.2	-82.6
27	**B**		8.11	1633	101.4	176.1	170	92	0.0	187.8	539.1	460.5	-	-80.5
35	**B**		8.16	428	54.3	39.6	35	15	0.0	90.4	41.5	197.4	-	-81.7
37	**B**		8.21	469	6.7	26.4	100	27	0.0	104.3	124.8	131.6	-	-79.9
46	**B**		8.19	617	58.0	35.2	100	27	0.0	146.0	170.0	153.5	-9.09	-74.6
36	**C**		8.22	337	32.6	33.0	28	28	0.0	132.1	40.0	109.7	-	-82.5
38	**C**		8.22	332	29.0	28.2	32	27	0.0	97.4	57.8	109.7	-	-81.5
40	**C**		8.19	421	40.1	36.6	32	28	0.0	104.3	123.0	109.7	-	-80.7

Table (1). Cont.

41	**C**		8.29	299	8.7	34.3	43	27	0.0	104.3	24.6	109.7	-	-81.8
42	**C**		8.3	461	43.5	39.6	44	47	0.0	205.1	75.2	109.7	-	-82.2
45	**C**		8.25	620	87.0	37.0	55	47	0.0	142.6	170.0	153.5	-9.26	-75.3
7	**D**		8.3	671	39.1	29.1	156	35	0.0	250.3	133.8	153.5	-	-81.7
15	**D**		8.2	444	30.4	23.8	75	31	0.0	233.0	80.0	87.7	-	-82.7
17	**D**		8.21	359	29.0	35.2	40	29	0.0	212.1	32.5	87.7	-	-83.3
19	**D**		8.3	524	34.8	44.9	82	25	0.0	257.3	121.5	87.7	-	-78.8
20	**D**		8.35	290	23.2	21.1	40	31	0.0	177.3	20.0	65.8	-	-81.7
21	**D**		8.21	431	29.0	35.2	75	26	0.0	250.3	52.4	87.7	-	-81
22	**D**		8.3	318	29.0	26.4	30	31	0.0	135.6	68.0	65.8	-	-82.3
26	**D**		8.22	218	17.4	24.7	12	30	0.0	97.4	20.0	65.8	-10.7	-80.1
Rain	--	Rainwater	7.0	29.15	7.1	0.6	2.3	Nil	Nil	14.5	6.4	5.5	-4.37	-

Table (2). Results of trace elements and radioactive nuclides in groundwater of the Nubian Sandstone aquifer in Kharga Oasis

Sample #	**Rb**	**Sr**	**Pb**	**^{232}Th**	**^{238}U**
			(ppb)		
3	29.13	798.20	1.80	0.118	0.009
4	18.06	1,415.2	20.19	0.117	6.314
5	8.24	366.13	3.03	0.064	0.016
6	19.00	493.85	0.46	0.053	0.009
8	13.65	359.42	0.25	0.028	0.009
11	20.10	402.54	0.15	0.033	0.100
13	15.15	370.87	0.06	0.021	0.009
18	64.83	2,906.0	1.03	0.026	9.424
25	50.81	1,437.88	0.29	0.003	0.037
23	51.17	985.88	1.13	0.007	0.009
30	34.97	1,027.71	8.52	0.022	0.013
33	31.03	1,146.47	3.44	0.000	0.003
2	30.00	905.89	0.88	0.215	0.009
10	15.64	294.80	0.93	0.03	0.009
16	26.42	726.021	3.69	0.037	0.004
27	20.13	4,570.47	0.261	0.011	0.457
35	33.65	1,149.21	4.16	0.003	0.009
36	36.9	1,416.39	4.78	0.041	0.009
40	17.12	1,391.32	8.41	0.127	0.676
22	86.06	1,392.18	5.17	0.058	0.872

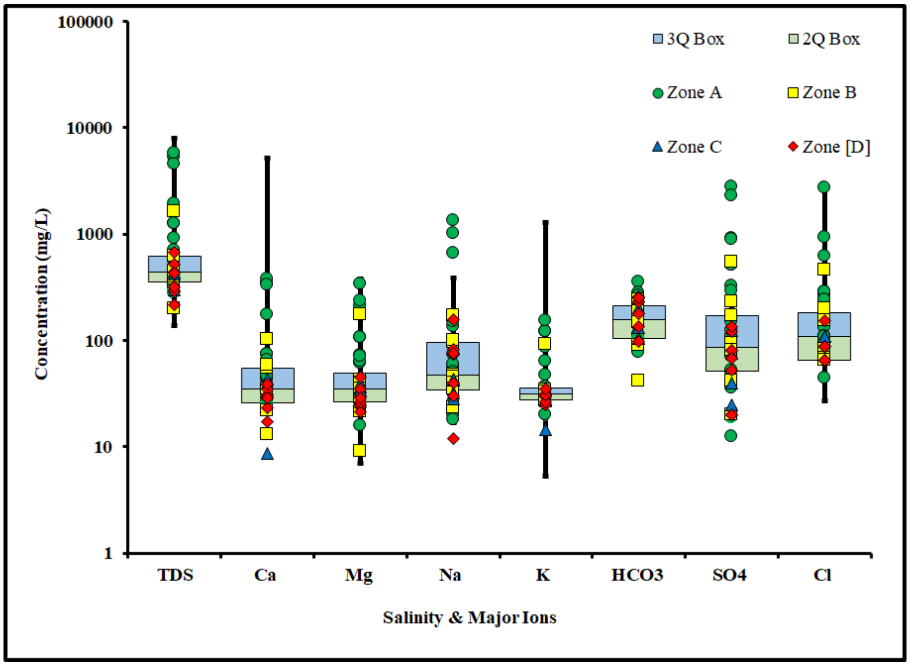

Fig. (3). A box plot of salinity and major ions concentrations in different aquifer zones of the Nubian Sandstone Aquifer in Kharag Oasis.

Most groundwater wells tapping the deep Six Hills formation (Zones C and D) record lower values of Ec, salinity, and lower concentrations of dissolved cations and anions; however, tapping the Taref formations (Zone A) records higher values. Like in Baharia Oasis as mentioned by El-Sayed et al. (2007) and Mosaad et al. (2022), the deeper groundwater zone of the NSA in Kharga possesses fresh groundwater type. On the other hand, the high concentrations of dissolved solids in Zone A are mainly due to water–rock interaction and irrigation return flux.

2. Geochemical Processes of Nubian Groundwater

The Piper Trilinear diagram has been used to investigate the geochemical processes affecting the groundwater quality in Kharga Oasis. In Fig. (4), all groundwater samples have been plotted where strong acids exceed weak acids (Areas 5, 6, 7, and 9). Six groundwater tapping Zone A (wells: 18, 24, 25, 28, 29, and 31) and two samples tapping Zone B (wells: 27 and 35) have been plotted in Area 6, revealing the Ca-Cl water type. Area 5 of the Piper diagram includes only one sample tapping Zone A (well 8) and three samples tapping Zone D (wells 7, 20, and 21), revealing Mg-HCO_3-type water. Area 7 includes seven groundwater samples: two from Zone A (wells: 4 and 33); three from Zone C (wells: 1, 14, and 35), and two from Zone D (wells: 7 and 15), representing the Na-Cl water type. The rest of groundwater samples have been plotted in the mixed region of the Piper diagram (Area 9). The Piper graph reveals that the groundwater of Zone D has been plotted in the lower part of Piper diagram in Areas # 5, 7, and 9, while most of the groundwater of Zone A has been plotted in the upper right corner of Area 6, and most of the groundwater samples tapping Zones B and C have been plotted in between Zones D and A. This indicates that groundwater geochemistry has evolved from the deeper Zone D to Zone A due to the water-rock interaction and upward leakages through fault planes revealed in the NSA as well as the impact of hydrothermal activities and confining conditions. The ion rations disclose the impact of geochemical processes on the groundwater quality. The groundwater alkalinity and chloride concentration correlate well with groundwater salinity (Fig. 5 a and b).

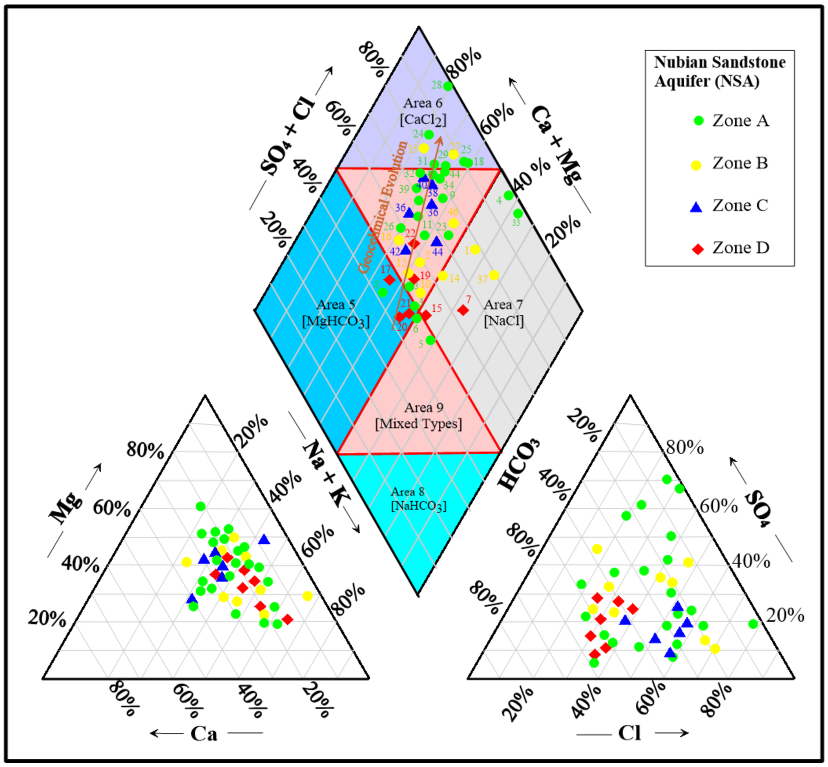

Fig. (4). Piper Trilinear diagram for groundwater samples tapping different aquifer zones in Khraga Oasis.

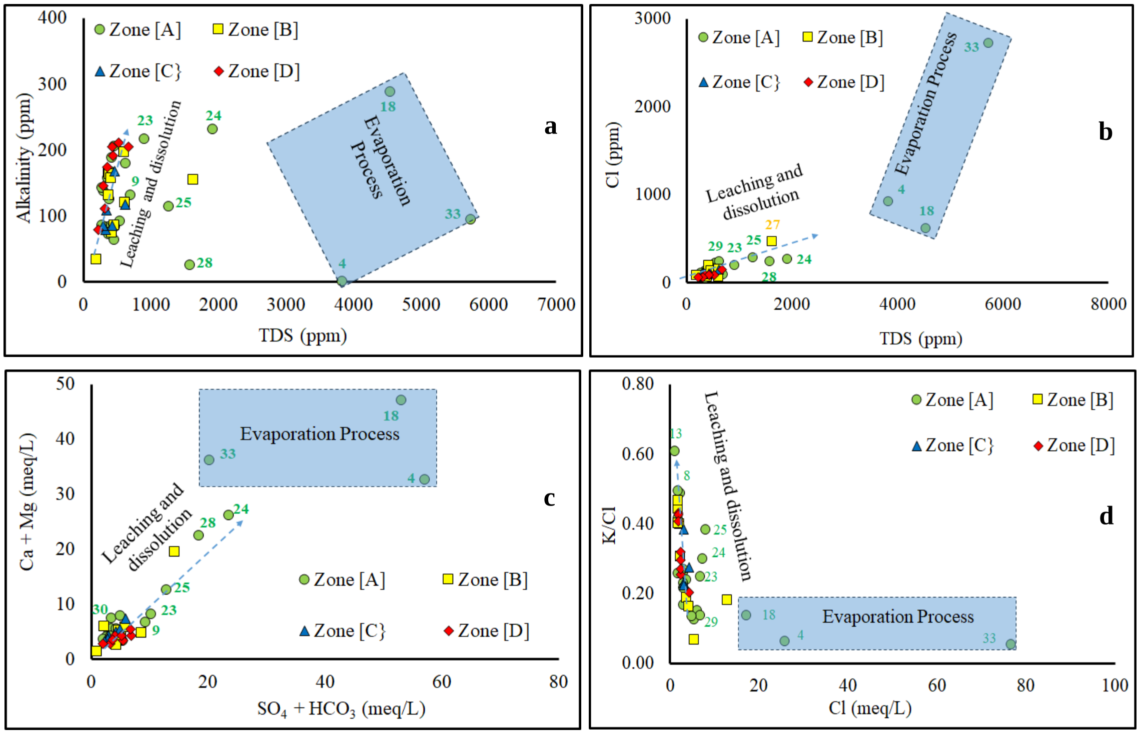

Fig. (5). Ion relationships show the main geochemical processes affecting the Nubian groundwater in Kharaga Oasis.

Additionally, SO_4 + HCO_3 is directly proportional with Ca + Mg and Cl inversely proportional with K/Cl (Fig. 5 c and d). Zones B, C and D normally have lower salinity and chloride, while the groundwater samples tapping Zone A record higher salinity and chloride concentration. Zone A typically plotted on the upper right side due to leaching and dissolution of the aquifer matrix and return flux from irrigation activities. However, shallow groundwater tapping Zone A (wells 4, 8, and 31) have deviated due to evaporation processes. These samples have Ca-Cl and Na-Cl water types.

3. Stable Isotopes and Origin of Groundwater

Stable isotopes affect groundwater recharge sources and provide significant insights into the geochemical processes affecting water quality (Samy et al., 2023 a, b). The stables isotopes ($\delta^{18}O$ and $\delta^{2}H$) are considered part of water molecules. $\delta^{18}O$ and $\delta^{2}H$ are important isotopic tracers frequently used in hydrogeology and environmental science to study and analyze groundwater systems (Craig, 1961 and Craig et al., 1963). Understanding groundwater's movement, sources, and age is crucial for effective resource management and environmental preservation (Eissa et al., 2013). The $\delta^{18}O$ in Kharga Oasis ranges between -11.96‰ (well 21) to -6.11‰ (well 33), while $\delta^{2}H$ ranges between -83.5‰ (well 10) to -67.7‰ (well 33) indicating paleo-groundwater. This coincided with the Sonntag report in 1986, where the groundwater in Kharga Oasis was initially supplied *in situ* during the humid pluvial periods (up to 30,000 years BP). The $\delta^{18}O$ and $\delta^{2}H$ isotopes can be found in varying proportions in groundwater that interacts with the aquifer environment, and they undergo distinct fractionation processes. By examining the isotopic composition of groundwater samples in Kharga Oasis, a wealth of information can be unraveled, such as the sources of recharge, the mixing of different water types, and the residence times of water within aquifers. In Fig. (6), the most depleted groundwater samples are collected from Zone D, while the most enriched are from Zone A. The shallow groundwater of Zone A (wells: 4, 18, 30, 33, and 43) and Zone B (wells: 2, 27, and 46) are mainly enriched due to evaporation processes because of irrigation water return that infiltrates that returns and recharges the shallow zone aquifer (Fig. 6 a and b). This has been confirmed by the relationship between the $\delta^{18}O$ and chloride, where chloride concentrations are increased with enrichments of $\delta^{18}O$. Chloride has been used as a conservative ion to illustrate the evolution of groundwater due to evaporation and water-rock interaction.

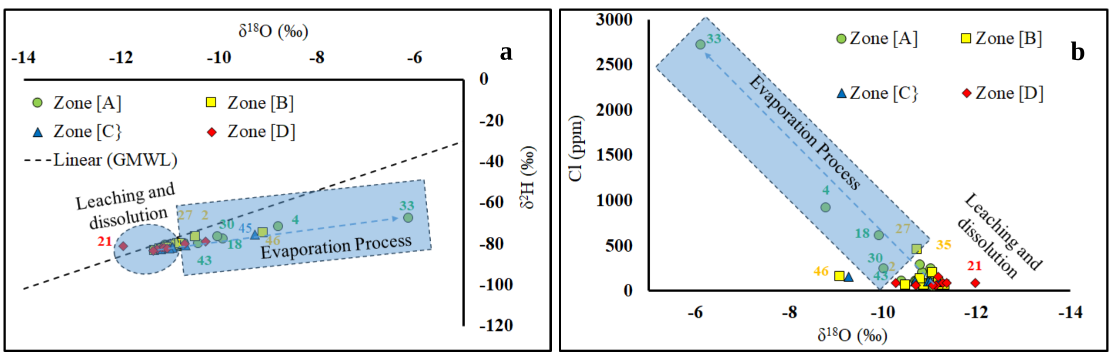

Fig. (6). Relationships between **a.** $\delta^{18}O$ and $\delta^{2}H$, **b.** Cl and $\delta^{18}O$ for the Nubian groundwater in Kharga Oasis.

The groundwater in Kharga Oasis explores the significance of $\delta^{18}O$ and $\delta^{2}H$ providing practical implications in managing groundwater resources and ensuring sustainable and secure water supply for both ecological and human needs. The stable isotopes ($\delta^{18}O$ and $\delta^{2}H$) indicate that the groundwater in the NSA is a deep confining fossil water that has a tremendous regional extension and was replenished thousands to millions of years ago by an intensification of paleo-monsoons (Sarnthein et al., 1981; Prell and Kutzbach, 1987; Yan and Petit-Maire 1994 and Mohamed et al., 2022). Therefore, monitoring groundwater quality and level fluctuation is crucial to assessing the sustainability of fossil nonrenewable groundwater as a sole public water supply source.

4. Trace and Radioactive Nuclides in the Nubian Groundwater

Investigating the radioactive nuclides in groundwater is vital for understanding the complex issues related to the movement of radioactive nuclides in groundwater, and for providing safe groundwater for human use. Researchers rely on such studies to develop strategies for monitoring, regulating, and mitigating the impact of radioactive contaminants in soil, rocks, and groundwater (Azeez et al., 2019; Belyaeva et al., 2019 and Wang et al., 2020). Radioactive nuclides in groundwater pose significant environmental and public health challenges due to their potential adverse effects. These nuclides can originate from natural sources, such as uranium and thorium, or anthropogenic activities, including nuclear power plants, mining operations, or industrial discharges. Monitoring and understanding the presence and behavior of these radioactive elements in groundwater is crucial to ensure the safety of drinking water supplies and minimize the health risks to communities. In Fig. (7), the Rb ranges from 8.24 ppb (well 5) to 86.06 ppb (well 22); Sr ranges from 294.8 (well 10) to 4570 (well 27). The ^{232}Th ranges from 0.003 ppb (well 33) to 0.21 ppb (well 2), and ^{238}U concentration in groundwater samples ranges between 0.003 ppb (well 33) and 9.42 ppb (well 18). The concentrations of ^{238}U and ^{232}Th are insignificant as they are within the range of permissible limits for human drinking based on WHO (2004).

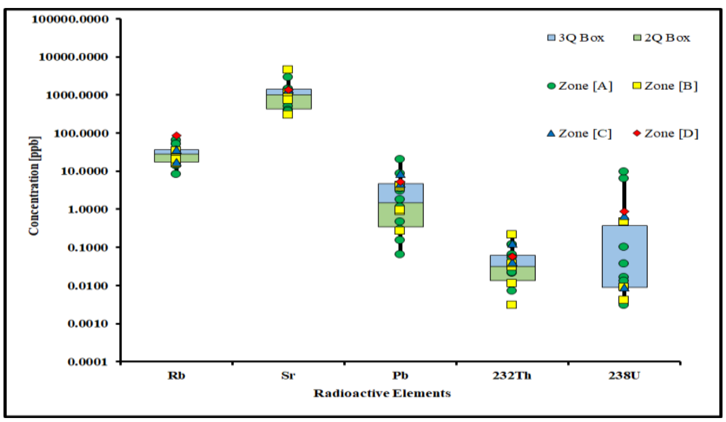

Fig. (7). Trace and radiogenic element concentrations in Kharga Oasis, Western Desert, Egypt.

In Fig. (8 a and b); the groundwater samples have relatively lower Sr, salinity, and depleted with the $\delta^{18}O$ are plotted on the more down left side, while samples of higher salinity and enriched with the $\delta^{18}O$ (Wells: 4, 8, and 33) are plotted in the upper right side (Fig. 8 a and b). These samples are shallow wells tapping Zone A of the NSA, which are affected by the return flux infiltration of irrigation drainage. Typically, the salinity arises, and the $\delta^{18}O$ is enriched due to evaporation processes.

In Fig. (8 b, c, and d), Sr are positively correlated with Rb, Pb, ^{232}Th (excluding samples that may experience evaporation; wells: 4, 8, 23, 25, 2, 33, and 35), indicating a geogenic source, which mainly due to leaching of granitic and basement rocks at the base of the NSA as well as clay sheets interbeds.

Higher concentrations of Sr and ^{238}U have been detected at wells 3 and 5, tapping to shallow Zone A (Fig. 8 f). The high concentrations are primarily seen in Zones A and B (shallow zones) than in Zones C and D (deeper zones) due to the impact of irrigation activities and intensive fertilizer uses. The radioactive nucleus accumulation from irrigation water is usually limited from the irrigation and Peddy-soil areas (Noli and Tsamos, 2018 and Huang et al., 2021). However, in arid climates during the summertime, the impact of leaching and evaporation probably increases the mobility of these nuclides to the groundwater. Additionally, higher radiogenicity has been declared from the intensive use of phosphate as fertilizer (Neiva et al., 2016 and Korany et al., 2021).

5. Geochemical NETPATH Reactive Model

The NETPATH model identifies the main processes affecting groundwater quality, including leaching/dissolution, evaporation, and mixing (Plummer et al., 1992). The geochemical model has been constrained by the minerals embedded in the NSA's aquifer matrix and the groundwater's geochemical analyses from different zones. Calcite, dolomite, and halite have been involved as phases as they are the dominant minerals in the soil and cementing materials of the aquifer matrix. Albite, alunite, anorthite, and chlorite have been involved as they are prevalent in the basement rocks, where the NSA rests over (Table 3). The saturation indices for the input constraints have been calculated using the WATEQ (Table 4). The geochemical model has coincided with the flow path and from more profound to the nearest shallow well to simulate the upward leakages. The NETPATH models simulate the evolution of Kharga Oasis's groundwater due to the aquifer matrix's leaching and dissolution with the subsurface flow bath and upward leakages from deeper to shallow zones. The models show dissolution/precipitation of calcite, dolomite, gypsum, silica, illite, albite, allunite, halite, and anorthite and precipitation of chlorite and evolving of CO_2 due to release pressure. The evaporation factors for samples tapping Zone A and Zone B (wells: 4, 9, 18, 30, 33, 43, 45 and 46) range from 1.3 (sample 9) to 2.89 (sample 33) from the original groundwater (Table 5). The evaporation factors were consistent and confirmed with the results that have been obtained from the stable isotopes.

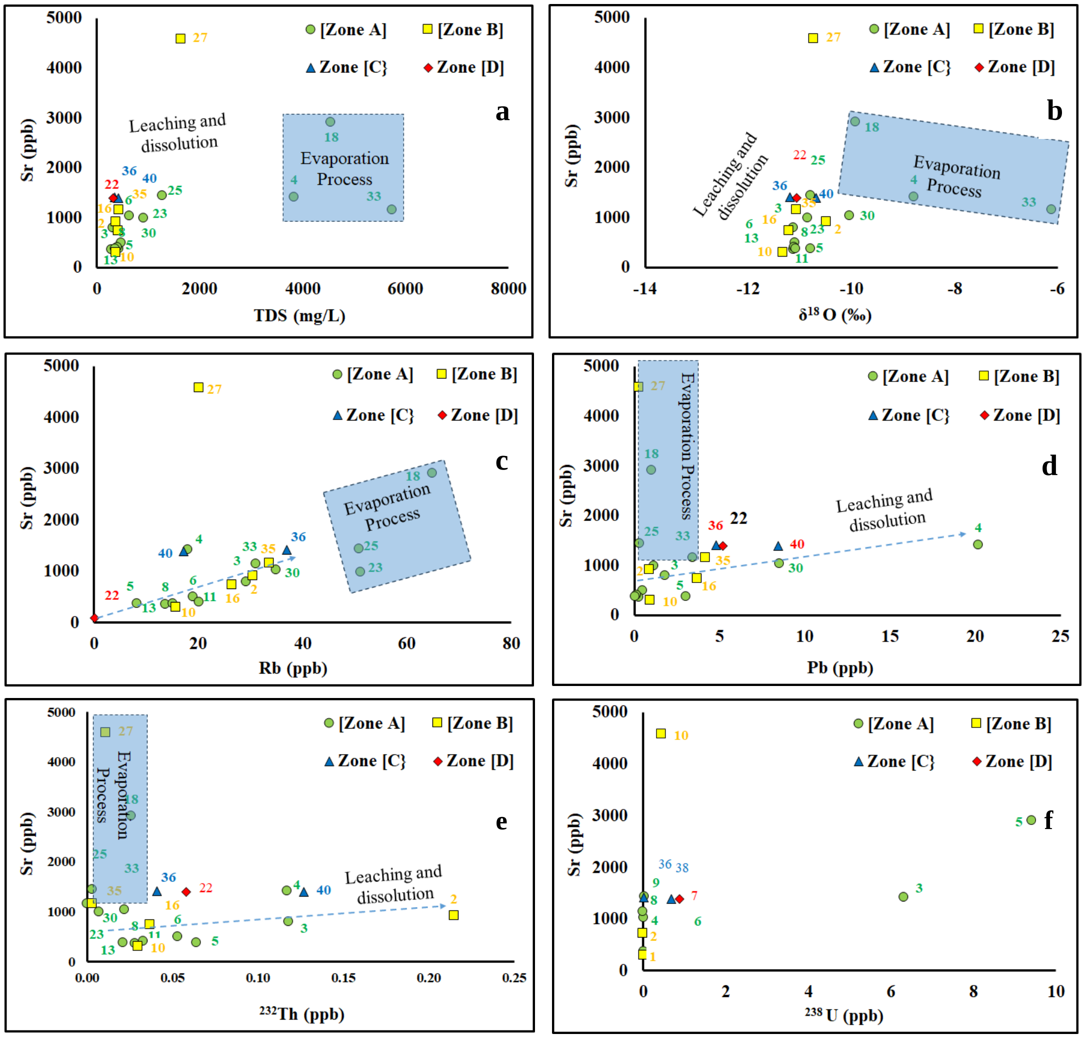

Fig. (8). Relationship between Sr with salinity, $\delta^{18}O$, and radiogenic nuclei.

Table (3). Mineral saturation indices for phases in NETPATH geochemical models.

Aquifer	Well no.	Cal.	Dol.	Gyp.	SiO_2	Alb	Alun	Anor	Chlr	Mica	Ca-Mont	Ilt	CO_2	Hal.
Nubbian Sandstone Aquifer (NSA)	**4**	-0.44	-0.88	-0.22	-1.01	1.09	3.44	0.60	5.28	13.78	5.19	6.20	-3.87	-0.50
	7	-0.45	-0.59	-1.99	-1.14	0.10	3.15	-0.48	-2.17	12.42	4.78	4.73	-1.52	-0.34
	8	0.05	0.17	-3.04	-1.03	1.16	-2.34	-0.07	2.23	12.23	5.03	5.09	-2.68	-0.28
	9	-0.15	0.27	-2.45	-0.98	2.33	-2.15	-0.33	5.81	12.01	4.47	5.07	-3.20	-2.37
	10	-0.17	0.22	-3.15	-1.07	1.55	-4.51	-0.81	4.92	10.46	3.26	3.72	-2.92	-2.41
	12	0.38	1.39	-2.26	-1.11	0.00	-3.63	-0.48	7.49	10.41	3.12	3.75	-2.86	-2.36
	16	-0.02	0.48	-2.21	-1.12	0.14	-0.95	-0.39	3.34	11.05	3.92	4.04	-2.25	-2.48
	17	0.41	1.34	-2.56	-1.13	-0.29	-3.93	-0.40	6.42	10.31	3.15	3.59	-2.60	-2.26
	18	0.88	2.00	-0.24	-1.02	0.80	4.17	0.66	5.27	13.92	5.53	6.34	-2.22	-0.05
	26	-0.71	-0.81	-3.03	-1.16	-0.15	-2.22	-0.78	1.51	10.21	3.65	3.33	-2.32	-0.31
	26	-0.71	-0.81	-3.03	-1.16	-0.15	-2.22	-0.78	1.51	10.21	3.65	3.33	-2.32	-2.74
	29	-0.68	-0.82	-2.04	-1.08	-0.21	3.18	-0.12	-0.42	13.03	5.67	5.46	-2.02	-3.59
	30	-0.23	0.18	-2.16	-1.08	-0.49	1.94	-0.16	1.44	12.69	5.28	5.28	-1.91	-2.54
	30	-0.23	0.18	-2.16	-1.08	-0.49	1.94	-0.16	1.44	12.69	5.28	5.28	-1.91	-2.62
	33	0.21	0.57	-0.63	-1.01	0.28	4.85	0.69	3.36	14.63	5.93	6.75	-2.52	-2.59
	33	0.21	0.57	-0.63	-1.01	0.28	4.85	0.69	3.36	14.63	5.93	6.75	-2.52	-2.79
	35	-0.46	-0.62	-2.35	-1.13	0.19	-0.18	-0.27	1.00	11.32	4.33	4.14	-2.29	-3.79
	40	-0.72	-1.06	-1.80	-1.13	-2.38	2.96	-0.29	-1.36	12.04	5.03	4.60	-1.89	-2.92
	40	-0.72	-1.06	-1.80	-1.13	-2.38	2.96	-0.29	-1.36	12.04	5.03	4.60	-1.89	-1.97
	45	0.26	0.54	-1.41	-1.11	-0.82	0.28	0.11	2.82	11.50	4.31	4.37	-2.39	-2.65
	46	0.10	0.36	-1.55	-1.10	-0.02		1.80	4.42	2.60	0.23	-2.97	-15.20	-2.69
	46	0.09	0.34	-1.57	-1.10	-0.49	0.27	-0.03	2.56	11.42	4.42	4.36	-2.38	-2.32

Note: Cal. Calcite; Dol. Dolomite; Gyp. Gypsum; Alb: Albite; Alun. Alunite; Anor. Anorthite; Chrt. Chlorite; Ca- mont. Ca-Montmorillonite; Ilt. Illite; Hal. Halite.

Table (4). Constraints, phases, and physical parameters used as input data in the NETPATH geochemical model.

Constrains	phases	Parameters
Calcium, Carbon, Chloride, Magnesium, Potassium, Sodium, Sulfur, Silica.	Calcite, Albite, Dolomite, Gypsum, SiO_2, Albite, Alunite, Anorth, Chlorite, K-Mica, Ca-MONT, Illite, NaCl, exchange,	Evaporation Ion Exchange

6. Geostatistical Analyses and Ions Source

The principal Component Analyses (PCA) have been employed to investigate the geochemical processes controlling the groundwater quality, considering the dissolved ions in groundwater as the main variables (Rao et al., 2007 and Ncibi et al., 2022). The PCA is a statistical technique used to reduce dimensionality and identify data patterns by transforming them into a new coordinate system (Fodor, 2002 and Li et al., 2017). In the context of groundwater analysis, PCA can be a valuable tool for several purposes: Researchers and hydrogeologists use PCA alongside other statistical and geostatistical techniques to better understand the complex dynamics of groundwater systems, identify sources of contamination, delineate groundwater flow patterns, and make informed decisions regarding water resource management and environmental protection (Machiwal and Jha 2015; Machiwal et al., 2018 and Trabelsi and Zouari, 2019). The Groundwater of Kharga datasets contain numerous variables (such as chemical concentrations, physical properties, etc.). PCA can help condense these variables into minor, uncorrelated variables (principal components) while retaining the most critical information. This dimensionality reduction can simplify the analysis and visualization of complex groundwater data.

PCA can reveal underlying patterns or relationships between different groundwater parameters. For instance, it can help identify clusters of variables that tend to vary together or highlight variables that contribute most significantly to the variability within the dataset. By reducing the dimensions of the data, PCA allows for easier visualization of groundwater data. It helps plot data points in a reduced-dimensional space, making understanding the relationships between different groundwater parameters easier. The PCA reveals 3-D component analyses that the physical parameters (EC TDS), major ions (Ca, Mg, Na, K, SO_4, Cl), radionuclides, and rare earth elements have been used as input data to the SPSS graphical user interface (Fig. 9). The results show the physical parameters and major ions (except HCO_3) have been plotted in one group that mainly

Table (5). NETPATH modeling results (mmol/L) for the Kharga Oasis. Positive values mean the phase is going into solution, while negative values mean the phase is being removed from the solution.

Area	Model type	Initial water	Final water	Cal.	Dol.	Gyp.	SiO_2	Alb	Alun	Anor	Chlr	Ilt	CO2	Hal.	Ex	Ev Factor
Nubian Sandstone Aquifer (NSA)	Reaction models	**7**	**4**	--	-2.75	22.67	--	-20.32	-2.68	-15.23		26.11	--	12.64	--	1.54
		12	**8**	-0.38		0.12	--	-21.53	-0.48	32.51	-0.13	--	--	0.001	31.91	--
		10	**9**	10.48	0.96	--	--	--	0.85	1.88	--	-1.09	-13.93	--	13.22	1.34
		10	**8**	--	--	--	--	--	--	--	--	--	--	--	--	--
		17	**18**	-4.21	0.55	0.27	--	-0.56	1.38	0.77	--	--	--	--	-3.23	1.32
		17	**16**	-0.86	0.29	0.50	--	10.02	0.005	15.03	--	--	--	0.01	14.81	--
		26	**30**	--	--	--	8.6	-28.72	0.11	0.05	-0.04		-0.65	--	--	2.4
		26	**33**	0.29	--	-0.4	8.85	-28.98	0.22	--	--	--	-0.61	0.49	--	2.89
		40	**45**	-0.29	--	--	--	-1.67	-0.08	2.48	-0.08	0.08	--	--	1.64	1.40
		40	**46**	-0.23	--	0.63		3.08	-0.32	0.04	-0.09	-2.41	--	--	--	1.4

Note: Cal. Calcite; Dol. Dolomite; Gyp. Gypsum; Alb: Albite; Alun. Alunite; Anor. Anorthite; Chrt. Chlorite; Ca- mont. Ca-Montmorillonite; Ilt. Illite; Hal. Halite.

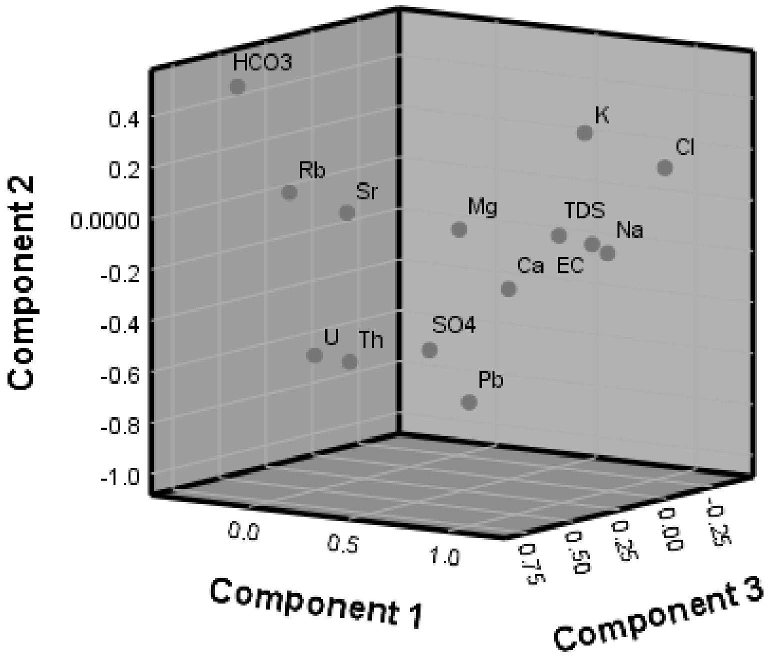

Fig. (9). Principal component analyses (PCA) for radiogenic, trace elements, and major ions dissolved in the Nubian groundwater.

characterizes the water-rock interaction with the aquifer matrix and evaporation process. Group II identified U, Th, Rb, Sr, and HCO_3, which are mainly controlled by the groundwater's pH values and redox potential.

CONCLUSION

Groundwater in Kharga Oasis, located in the Western Desert of Egypt, is an essential resource for the local population. Kharga Oasis is characterized by an arid climate where high temperature and scarce rainfall are the prevailing climates. The oasis is fed by the Nubian Sandstone Aquifer (NSA) of the Cretaceous age, one of the world's largest aquifers, providing freshwater for drinking, irrigation, domestic use, and industrial purposes. The NSA possesses three bearing formations; Taref (Zone A), Sabaya (Zone B), and Six Hills (Zones C, and D), which are separated by clay confining layers; the total penetration depth ranges from 12.5 to 800 meters and overlain the granitic and basement rocks. Aquifer management and conservation measures are crucial to reducing the impact of over-extraction and protecting groundwater quality from further degradation. Forty-six groundwater samples were collected in the summer of 2022 for major ions, radioactive elements, and stable isotope analyses to investigate the geochemical processes deteriorating the groundwater quality and determining the groundwater recharge source. The groundwater temperature ranges between 18 to 36.8°C, where high temperatures have been detected in deeper zones (Zones C and D), indicating geothermal activity. Most of the groundwater samples of the NSA are fresh to brackish water types, and the deep aquifer (zones C and D) possesses freshwater. The NSA does not contain significant concentrations of the natural radioactive nuclei, including Rb, Sr, Pb, Th, and Sr. The lower concentrations were detected in deeper zones that do not exceed the permissible drinking limits. The concentrations were elevated in the uppermost shallow aquifer zone mainly due to the geogenic sources from the basal basement rocks and anthropogenic activities. The stable isotopes ($\delta^{18}O$ and $\delta^{2}H$) show great insights for recharge and salinization sources. The $\delta^{18}O$ ranges from -11.96 to -6.11‰, while $\delta^{2}H$ ranges between -83.5‰ (Well10) to -67.7‰, indicating that NSA is fossil water where the aquifer has received a paleo recharge within a paleo-wet paleoclimate. The depleted values have been recorded in the deeper horizons (C and D) and enriched in the shallow aquifer zones (A and B). These geochemical and isotopic data analyses have been used as input for the NETPATH model and the Principal Component Analyses (PCA) to investigate factors deteriorating the groundwater quality. The geochemical NETPATH model shows that water-rock interaction with aquifer matrix and evaporation processes are the main factors that deteriorate groundwater quality in the upper zone. The upward leakages through the fault plain from deeper zones and return fluxes from irrigation in the shallow aquifer zones (Zone A) affect the groundwater quality and lead to groundwater salinization. The principal component analyses (PCA) show two groundwater groups: Group I includes salinity and major ions, which are mainly affected by the leaching of minerals forming the aquifer matrix, and Group II, controls by the alkalinity and radioactive nuclei (Rb, Sr, Pb, Th, and Sr) due to the prevailing of oxidation and reduction processes because of geothermal activity. The groundwater in Kharga Oasis is a paleo nonrenewable source and is quality threatened mainly by geogenic natural pollution, agricultural activity, and over-exploitation.

REFERENCES

Abd Allah, H.F. (2013). Environmental impacts of over exploitation on the nubian sandstone aquifer in some localities, North El Kharga Oasis, Western desert, Egypt. M.Sc. Thesis, Department of Geology, Menoufia University, Faculty of Science, 127 p.

Ammar, F.H., P. Deschamps, N. Chkir, K. Zouari, A. Agoune and B. Hamelin (2020). Uranium isotopes as tracers of groundwater evolution in the Complex Terminal aquifer of southern Tunisia. Quaternary International, 547: 33-49.

Argyrous, G. (20110. In: ‘Statistics for Research: With A guide to SPSS’. 3rd Ed., pp.1-608.

Azeez, H.H., H.H. Mansour and S.T. Ahmad (2019). Transfer of natural radioactive nuclides from soil to plant crops. Applied Radiation and Isotopes, 147: 152-158.

Belyaeva, O., K. Pyuskyulyan, N. Movsisyan, et al. (2019). Natural radioactivity in urban soils of mining centers in Armenia: dose rate and risk assessment. Chemosphere, 225: 859–870.

Boukhary, M., M.E.A. Bassiouni, B. Issawi, S. Sharabi and H. Mansour (2013). Maastrichtian–early Paleogene Ostracoda from the Kharga Oasis and the Nile Valley, Egypt. Micropaleontology, 59: 223-248.

CONOCO (1987). Geological map of Egypt (scale 1:500,000).

Coplen, T.B. (1995). Reporting of stable hydrogen carbon and oxygen isotopic abundances. Geothermics, 24: 707–712.

Coplen, T.B., J.D. Wildman and J. Chen (1991). Improvements in the gaseous hydrogenwater equilibrium technique for hydrogen isotope ratio analysis. Analytical Chemistry, 63: 910–912.

Craig, H. (1961). Isotopic variations in meteoric waters. Science, 133: 1702–1703.

Craig, H., L.I. Gordon and Y. Horibe (1963). Isotopic exchange effects in the evaporation of water: 1. Low-temperature experimental results. Journal of Geophysical Research, 68 (17): 5079-5087.

Diab, M.Sh. (1978). A regional hydrogeological study of artesian water aquifer in the Western Desert of Egypt. Symposium on the geology of Middle East, Anqara, Turkey.

Divers, M.T., E.M. Elliott and D.J. Bain (2014). Quantification of nitrate sources to an urban stream using dual nitrate isotopes. Environmental Science and Technology, 48 (18): 10580-10587.

Eissa, M.A., J.M. Thomas, R.L. Hershey, M.I. Dawoud, G. Pohll, M.A. Gomaa and A.D. Kamal (2013). Geochemical and isotopic evolution of groundwater in the Wadi Watir Watershed, Sinai Peninsula, Egypt. Environmental Earth Sciences, 71. DOI:10.1007/s12665-013-2588-4.

El-Sankary, M.M. (2002). Geological, sedimentological and radioactivity studies of the quaternary sediments, El Kharga Depression, Western Desert, Egypt. Ph.D. Thesis, Ain Shams Univ., Cairo, Egypt, 241 p.

El-Sayed, M.H., H.A. Shawky and H. Ibrahim (2007). Chemical and geothermal studies on the groundwater of Dakhla Oasis, Western desert, Egypt. Ain Shams Science Bulletin, 45: 57-88.

FAO (1977). Groundwater Pilot Scheme, New Valley, Egypt. Agricultural Development Prospects in the New Valley: Rome, EGY 71/561, Technical Report no. 4.

Fodor, I.K. (2002). A survey of dimension reduction techniques. Technical Report No. UCRL-ID-148494. United States, DOI: 10.2172/15002155.

Hellström, B. (1940). The subterranean water in the Libyan Desert. Geografiska Annaler, 22 (3-4): 206-239.

Hem, J.D. (1985). Study and interpretation of the chemical characteristics of natural water (Vol. 2254). Department of the Interior, US Geological Survey.

Huang, Y.J., L.T. Yang, F. Zhao, et al. (2021). Spatial distribution and characteristic of radiological hazard of the paddy field around a decommissioned uranium mine in eastern China. Journal of Radioanalytical and Nuclear Chemistry, 327 (4): 789–799.

Islam, A.R.M.T., N. Ahmed, M. Bodrud-Doza and R. Chu (2017). Characterizing groundwater quality ranks for drinking purposes in Sylhet district, Bangladesh, using entropy method, spatial autocorrelation index, and geostatistics. Environmental Science and Pollution Research, 24: 26350-26374.

King-Okumu, C., A. Abdelkhalek and B. Salem (2021). Characterizing Ecosystem Services to Human Well-Being in Groundwater Dependent Desert Environments. In: 'Groundwater in Egypt's Deserts', Springer, pp. 79-101.

Klitszch, E., F.K. List and G. Pohlmann (1987). Geological Map of Egypt, sheet NG36Sw - Luxor, 1:500,000. Cairo: Conoco Coral-Egyptian General Petroleum Company.

Korany, K.A., A.M. Masoud, O.E. Rushdy, Z.A. Alrowaili, F.H. Hassanein and M.H. Taha (2021). Phosphate, phosphoric acid and phosphogypsum natural radioactivity and radiological hazards parameters. Journal of Radioanalytical and Nuclear Chemistry, 329 (1): 391-399.

Lamoreaux, P.E., B.A. Memon and H. Idris (1985). Groundwater development, Kharga Oases, Western Desert of Egypt: a long-term environmental concern. Environmental Geology and Water Sciences, 7: 129-149.

Li, H., J. Liu, R.W. Liu, N. Xiong, K. Wu and T.H. Kim (2017). A dimensionality reduction-based multi-step clustering method for robust vessel trajectory analysis. Sensors, 17 (8): 1792.

Machiwal, D. and M.K. Jha (2015). Identifying sources of groundwater contamination in a hard-rock aquifer system using multivariate statistical analyses and GIS-based geostatistical modeling techniques. Journal of Hydrology: Regional Studies, 4: 80-110.

Machiwal, D., V. Cloutier, C. Güler and N. Kazakis (2018). A review of GIS-integrated statistical techniques for groundwater quality evaluation and protection. Environmental Earth Sciences, 77: 1-30.

Mahmod, W.E., K. Watanabe and A.A. Zahr-Eldeen (2013). Analysis of groundwater flow in arid areas with limited hydrogeological data using the Grey Model: a case study of the Nubian Sandstone, Kharga Oasis, Egypt. Hydrogeology Journal, 21 (5): 1021.

Mekkawi, M., T. Arafa-Hamed, P. Amatykul, M. Atya and Y. Ogawa (2017). Three-dimensional modelling of Kharga reservoir water, New Valley-Egypt, using magnetotelluric data. Journal of Geology and Geophysics, 7 (318): 2.

Mishra, U., A.K. Mohapatra, A. Mandal and A. Singh (2023). Identification of potential artificial groundwater recharge sites in an alluvial setting: a coupled electrical resistivity tomography and sediment characterization study. Groundwater for Sustainable Development, 20: 100875.

Mohamed, A., E. Ahmed, F. Alshehri and A. Abdelrady (2022). The groundwater flow behavior and the recharge in the Nubian sandstone aquifer System during the wet and arid periods. Sustainability, 14 (11): 6823.

Mondal, B.K., S. Sahoo, R. Das, P.K. Mishra, K. Abdelrahman, et al. (2022). Assessing groundwater dynamics and potentiality in the lower ganga plain, India. Water, 14 (14): 2180.

Mosaad, S., M. Eissa and A.K. Alezabawy (2022). Geochemical modeling and geostatistical categorization of groundwater in Nubian Sandstone Aquifer, El Bahariya Oasis, Egypt. Environmental Earth Sciences 81: 421.

Mukate, S.V., D.B. Panaskar, V.M. Wagh and S.J. Baker (2020). Understanding the influence of industrial and agricultural land uses on groundwater quality in semiarid region of Solapur, India. Environment, Development and Sustainability, 22: 3207-3238.

Ncibi, K., M. Mastrocicco, N. Colombani, G. Busico, R. Hadji, Y. Hamed and K. Shuhab (2022). Differentiating nitrate origins and fate in a semi-arid basin (Tunisia) via geostatistical analyses and groundwater modelling. Water, 14 (24): 4124.

Neiva, A.M.R., I.M.H.R. Antunes, P.C.S. Carvalho and A.C.T. Santos (2016). Uranium and arsenic contamination in the former Mondego Sul uranium mine area, Central Portugal. Journal of Geochemical Exploration, 162: 1-15.

Noli, F. and P. Tsamos (2018). Seasonal variations of natural radionuclides, minor and trace elements in lake sediments and water in a lignite mining area of North-Western Greece. Environmental Science and Pollution Research, 25 (13): 12222–12233.

Plummer, L.N., E.C. Prestemon and D.L. Parkhurst (1992). NETPATH: An interactive code for interpreting NET geochemical reactions from chemical and isotopic data along a flow PATH. Water-rock interaction, Rotterdam, Balkema, pp. 239–242.

Prell, W.L., J.E. Kutzbach (1987). Monsoon variability over the past 150,000 years. Journal of Geophysics Research-Earth Surface, 92: 8411–8425.

Rao, N.S., J.P. Rao and A. Subrahmanyam (2007). Principal component analysis in groundwater quality in a developing urban area of Andhra Pradesh. Geological Society of India, 69 (5): 959-969.

RIGW (2006). Southern Egypt Development Project. Research Institute for Ground Water, unpublished internal report, 16 p.

Saber, M., M. Mokhtar, A. Bakheit, A.M. Elfeky, M. Gameh, A. Mostafa, A. Sefelnasr, S.A. Kantoush, T. Sumi, T. Hori and A. Hamada (2022). An integrated assessment approach for fossil groundwater quality and crop water requirements in the El-Kharga Oasis, Western Desert, Egypt. Journal of Hydrology: Regional Studies, 40: 101016.

Samy, A., M. Eissa, S. Shahen, M.M. Said and R.M. Abou Shahaba (2023a). Geochemistry and assessment of groundwater resource in coastal arid region aquifer (Dahab delta, South Sinai, Egypt). Beni-Suef University Journal of Basic and Applied Sciences, 12 (1): 1-21.

Samy, A., M. Eissa, S. Shahen, M.M. Said and R.M. Abou Shahaba (2023b). Solute transport and geochemical modeling of the coastal quaternary aquifer, Delta Dahab Basin, South Sinai, Egypt. Acta Geochimica, 1-24.

Sarnthein, M., G. Tetzlaff, B. Koopmann, K. Wolter and U. Pflaumann (1981). Glacial and interglacial wind regimes over the eastern subtropical Atlantic and North-West Africa. Nature, 293: 193–196.

Sherif, M.I. and N.C. Sturchio (2021). Elevated radium levels in Nubian Aquifer groundwater of Northeastern Africa. Scientific Reports, 11 (1): 78.

Sinha, H., S.C. Rai and S. Kumar (2023). Post-monsoon groundwater hydrogeochemical characterization and quality assessment using geospatial and multivariate analysis in Chhotanagpur Plateau, India. Environment, Development and Sustainability, DOI: 10.1007/s10668-023-03459-8.

Soliman, S.M. (2013). Mitigation of excessive drawdowns via rotational groundwater withdrawal (Case study: El Kharga Oases, Egypt). New York Science Journal, 6/1: 118–123.

Sonntag, C. (1986). A time-dependent groundwater model for the Eastern Sahara. Berliner Geowissenschaftlichen Abhandlungen, A72: 124–134.

Trabelsi, R. and K. Zouari (2019). Coupled geochemical modeling and multivariate statistical analysis approach for the assessment of groundwater quality in irrigated areas: A study from North Eastern of Tunisia. Groundwater for Sustainable Development, 8: 413-427.

Uddin, M.G., M.T.M. Diganta, A.M. Sajib, M.A. Hasan, M. Moniruzzaman, A. Rahman, A.I. Olbert and M. Moniruzzaman (2023). Assessment of hydrogeochemistry in groundwater using water quality index model and indices approaches. Heliyon, 9 (9): e19668.

Wang, R., J. Mai, Y. Guan, et al. (2020). Radionuclides in the environment around the uranium mines in Guangxi, China. Applied Radiation and Isotopes, 159: 109098.

WHO (2004). In: ‘Guidelines for Drinking Water Quality: Radiological Aspects. 3rd Ed. World Health Organization, Geneva.

Yan, Z. and N. Petit-Maire (1994). The last 140 ka in the Afro-Asian arid/semi-arid transitional zone. Palaeogeography, Palaeoclimatology, Palaeoecology, 110: 217–233.

Younis, A., M. Soliman, S. Moussa, U. Massoud, S. Abd ElNabi and M. Attia (2016). Integrated geophysical application to investigate groundwater potentiality of the shallow Nubian aquifer at northern Kharga, Western Desert, Egypt. NRIAG Journal of Astronomy and Geophysics, 5 (1): 186-197.

دلائل جيوكيميائية وإشعاعية ونظائرية لتقييم المياه الجوفية بالحجر الرملي النوبي بواحه الخارجة – الصحراء الغربية – مصر

مصطفى عبد الله عيسى
قسم الهيدروجيوكيمياء، مركز بحوث الصحراء، المطرية، القاهرة، مصر

تعتبر المياه الجوفية بخزان الحجر الرملي النوبي في واحة الخارجة والتي تقع في جنوب الصحراء الغربية المورد الرئيسي والأوحد للسكان. يعتبر الخزان النوبي من أكبر خزانات المياه الجوفية في العالم، والتي توفر مصدرًا للمياه العذبة للشرب والري والاستخدام المنزلي والأغراض الصناعية. يتكون هذا الخزان من ثلاث طبقات منتجة وهي من أعلى الى أسفل الطارف والصبايا والتلال الستة والتي تفصل بينها طبقات طينية مكونه خزان جوفي محبوس. يتراوح عمق الخزان من ١٢.٥ إلى ٨٠٠ متر تقع الصخور الجرانيتية أسفل الخزان مكونة سطح عدم توافق. تتراوح درجة حرارة المياه الجوفية بين ١٨ إلى ٣٦.٨ درجة مئوية، حيث تم اكتشاف درجات حرارة مرتفعة في المناطق الأعمق خاصة النطاث C وD، مما يشير إلى أن النشاط الحراري الأرضي ينشط مع العمق. معظم عينات المياه الجوفية في الخزان تحتوي على مياه عذبة إلى قليلة الملوحة، وتمتلك طبقة المياه الجوفية العميقة C وD مياه عذبة جدًا. لا تحتوي NSA على تركيزات كبيرة من العناصر المشعة الطبيعية، بما في ذلك Rb وSr وPb وTh وSr حيث لا تتجاوز الحدود المسموح بها للشرب. أثبتت النظائر الثابتة $\delta^{18}O$ و$\delta^{2}H$ أن المياه الجوفية في جميع الطبقات للخزان النوبي غير متجددة. يتراوح $\delta^{18}O$ من -١١.٩٦ إلى -٦.١١‰، بينما يتراوح $\delta^{2}H$ بين -٨٣.٥‰ (رقم 10) إلى -٦٧.٧‰، مما يشير إلى أن NSA عبارة عن مياه أحفورية حيث تلقت طبقة المياه الجوفية إعادة شحن خلال مناخ قديم لعصور جيولوجية رطبة باردة. تعتبر المياه الجوفية في واحة الخارجة مصدرًا غير متجدد، ونوعيتها مهددة بشكل رئيسي بالتلوث الطبيعي الجيولوجي، والنشاط الزراعي، والاستغلال المفرط.